national accelerator laboratory

NAL-Conf-73/25-EXP
7200.141

(Presented at the International Conference
on High Energy Particle Collisions,
Vanderbilt University, Nashville, Tennessee,
March 1973)

pp INTERACTIONS AT 205 GeV/c

S. Barish, Y. Cho, D. Colley, M. Derrick, R. Engelmann,
T. Fields, L. Hyman, K. Jaeger, B. Musgrave, J. Phelan,
J. Rest, P. Schreiner, P. Schultz, R. Singer, and H. Yuta
Argonne National Laboratory, Argonne, Illinois 60439 USA

and

L. Voyvodic, R. Walker, and J. Whitmore
National Accelerator Laboratory, Batavia, Illinois 60510 USA

June 1973

pp INTERACTIONS AT 205 GeV/c

Argonne-NAL Collaboration*
presented by

J. Whitmore
National Accelerator Laboratory
Batavia, Illinois 60510

ABSTRACT

Preliminary results are presented on 205 GeV/c pp interactions in the 30-inch hydrogen bubble chamber. The single particle inclusive distributions are compared to other NAL data, ISR data, and data from lower energies. Data on charged particle correlations and the preliminary results of a study of the diffractive process are also discussed.

In this report we will present some new results from a 50,000 picture exposure of the 30-inch bubble chamber to a 205 GeV/c proton beam at the National Accelerator Laboratory. The total number of interactions observed is 8828 (without corrections to the two-prong sample for azimuthal and small t scanning losses) and corresponds to 235 events/mb. The charged particle multiplicity parameters are presented in Table I and are in excellent agreement with those previously published[1] by this collaboration using approximately one-third of the present data. The errors, however, have been reduced by ~30%.

---

*S. Barish, Y. Cho, D. Colley, M. Derrick, R. Engelmann, T. Fields, L. Hyman, K. Jaeger, B. Musgrave, J. Phelan, J. Rest, P. Schreiner, P. Schultz, R. Singer, H. Yuta, L. Voyvodic, R. Walker, and J. Whitmore

TABLE I

	All Prongs	Negatives
Modal (Peak)	5.99 ± 0.03	--
Median	7.13 ± 0.11	--
Mean $<n>$	7.68 ± 0.11	2.84 ± 0.06
$<n(n-1)>$	66.6 ± 1.5	9.05 ± 0.23
$<n(n-1)(n-2)>$	636 ± 17	30 ± 1
f_2	7.66 ± 0.49	1.00 ± 0.14
f_3	7.25 ± 1.9	-1.09 ± 0.31

Measurements have been performed on a sample of events in order to study a) the inclusive distributions of particle production, b) the structure of individual events, and c) the diffractive excitation of target and projectile. For this high beam momentum and for high multiplicity events, there are practical complications to the measurement of momenta and angles of secondary tracks in a small bubble chamber. These problems involve track matching in the different stereoscopic views, overlapping track images, and poor momentum determination for fast forward-going secondaries. To investigate the effects of these complications, we have made two independent measurements. The first method involves using the uniqueness of the spatial pattern of the bubbles to match all secondary tracks. The second method involves measuring only those tracks consistent with particle production in the backward CM hemisphere.[2] The number of events analyzed by each method was 440 and 1484 respectively. The two methods yielded compatible results in a track by track comparison as well as compatible distributions for the entire sample.

To obtain π^- distributions, we have used a simple Monte-Carlo technique to estimate the effects of the K^- and $\bar{p}$ contamination. We tried several functional forms for the K^- and $\bar{p}$ invariant cross sections with intensities of 7% K^-'s and 2% $\bar{p}$'s in the Monte-Carlo generation. We interpret the generated tracks as π^-, apply the corrections to the raw negative particle spectra, and obtain the π^- inclusive distributions. The resulting corrections[3] were insensitive to reasonable variations of the shape of the K^- and $\bar{p}$ spectra and are shown in Fig. 1.

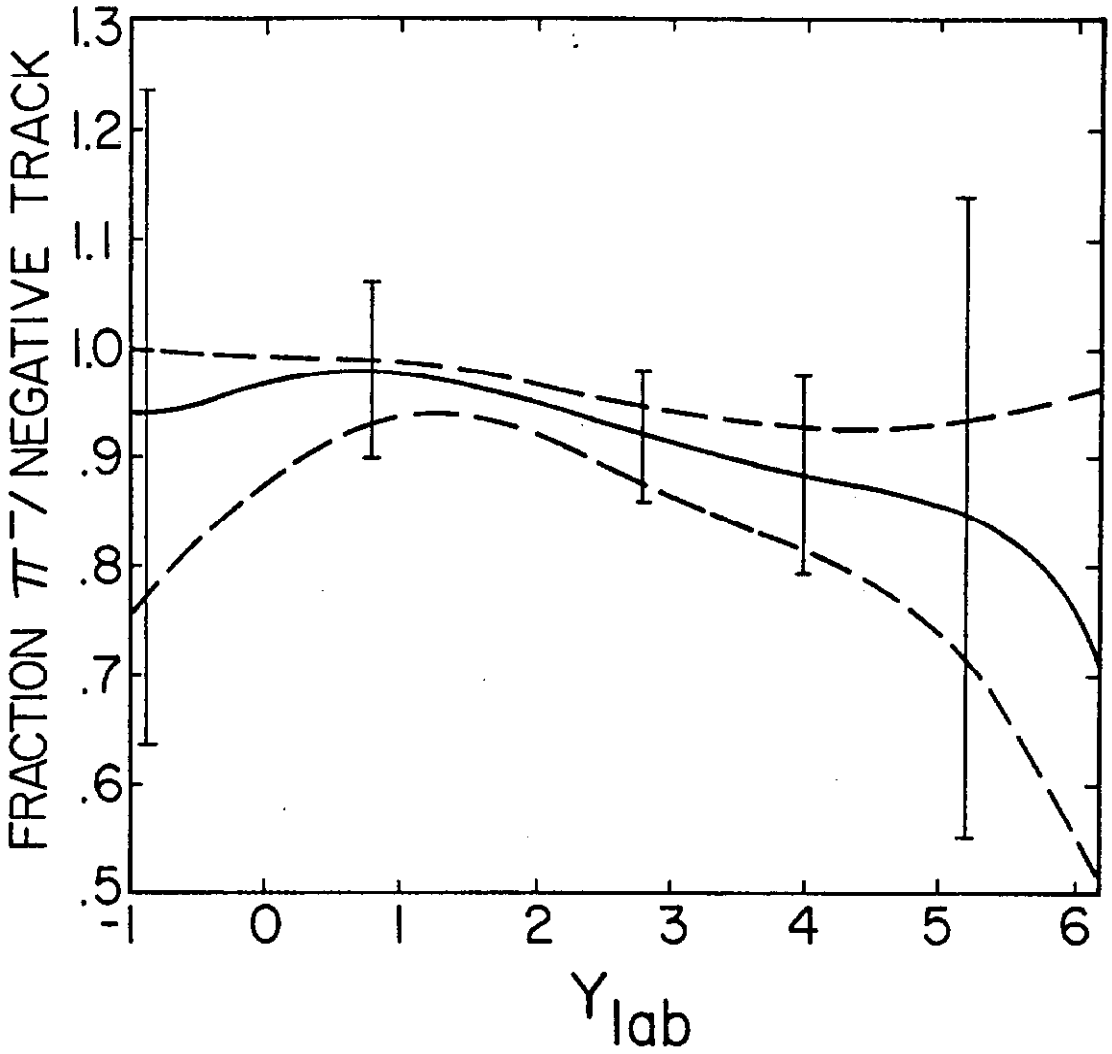

Fig. 1 Corrections applied to the raw negative particle rapidity distribution to obtain π^- spectra at 205 GeV/c. The error bars show the statistical errors on the raw data.

Data on $\pi^\pm$ production have also been obtained[4] from the 102 and 303 GeV/c bubble chamber experiments. Shown in Fig. 2 are the x distributions for $\pi^\pm$ production for various values of the transverse momentum p_T. Figure 3 shows the x distributions obtained by integrating over all p_T^2. These data are compared to lower energy data[5] as well as to ISR data.[6] p_T^2 distributions for π^- production for various x intervals and when integrated over all x are shown in Fig. 4.

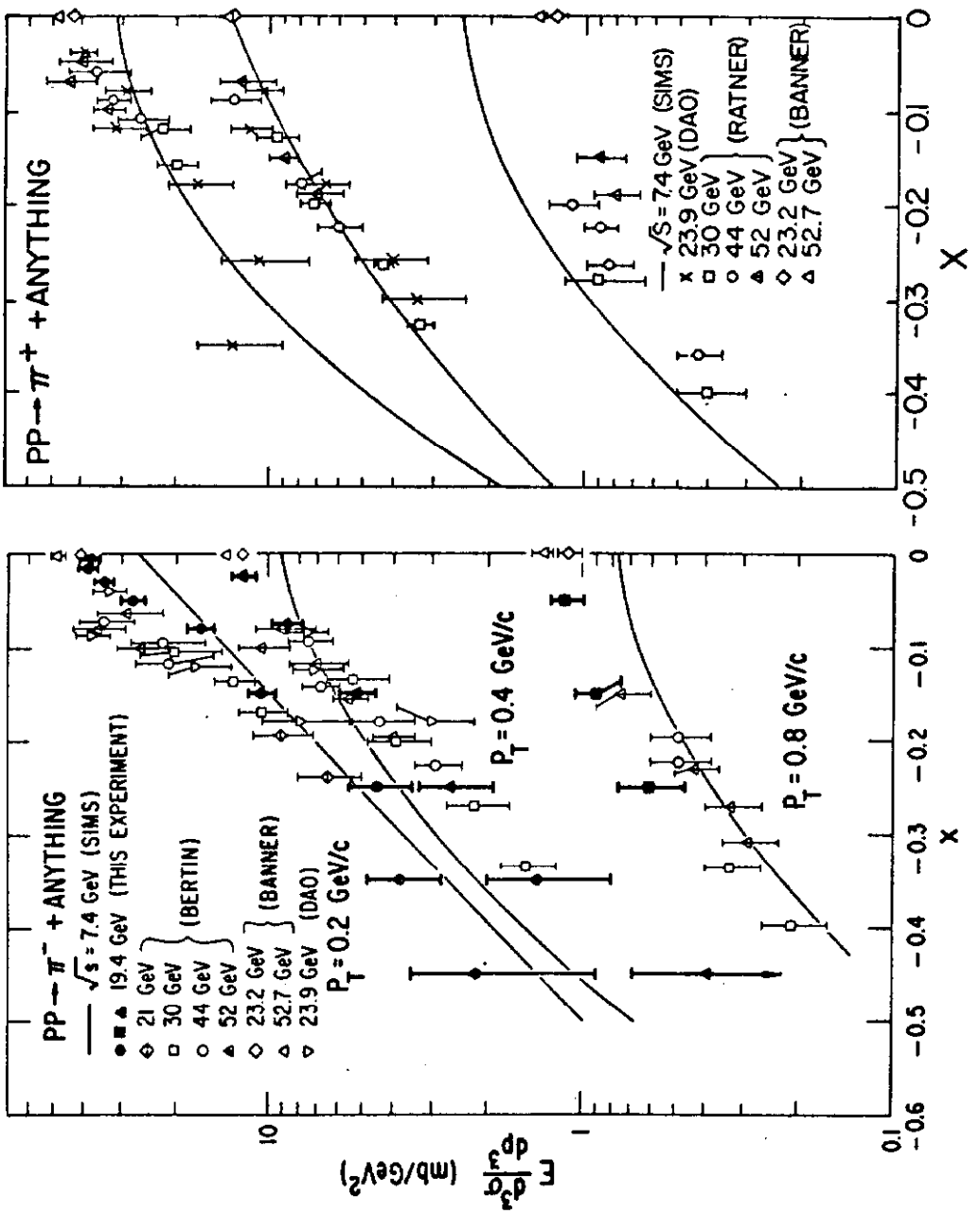

Fig. 2 x distributions for $\pi^{\pm}$ production at p_T = 0.2, 0.4, and 0.8 GeV/c.

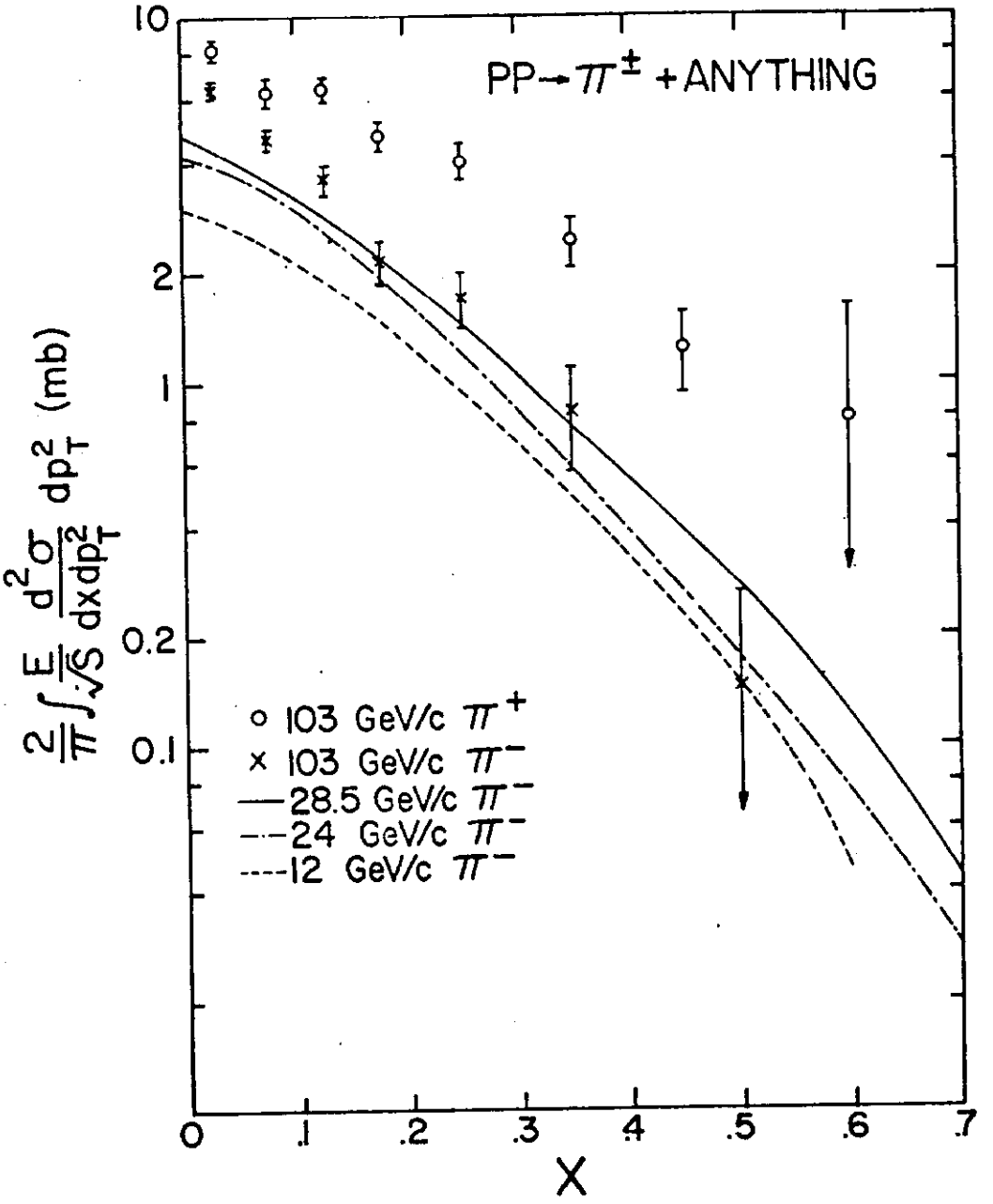

Fig. 3 x distributions for $\pi^{\pm}$ production obtained after integrating over all p_T^2.

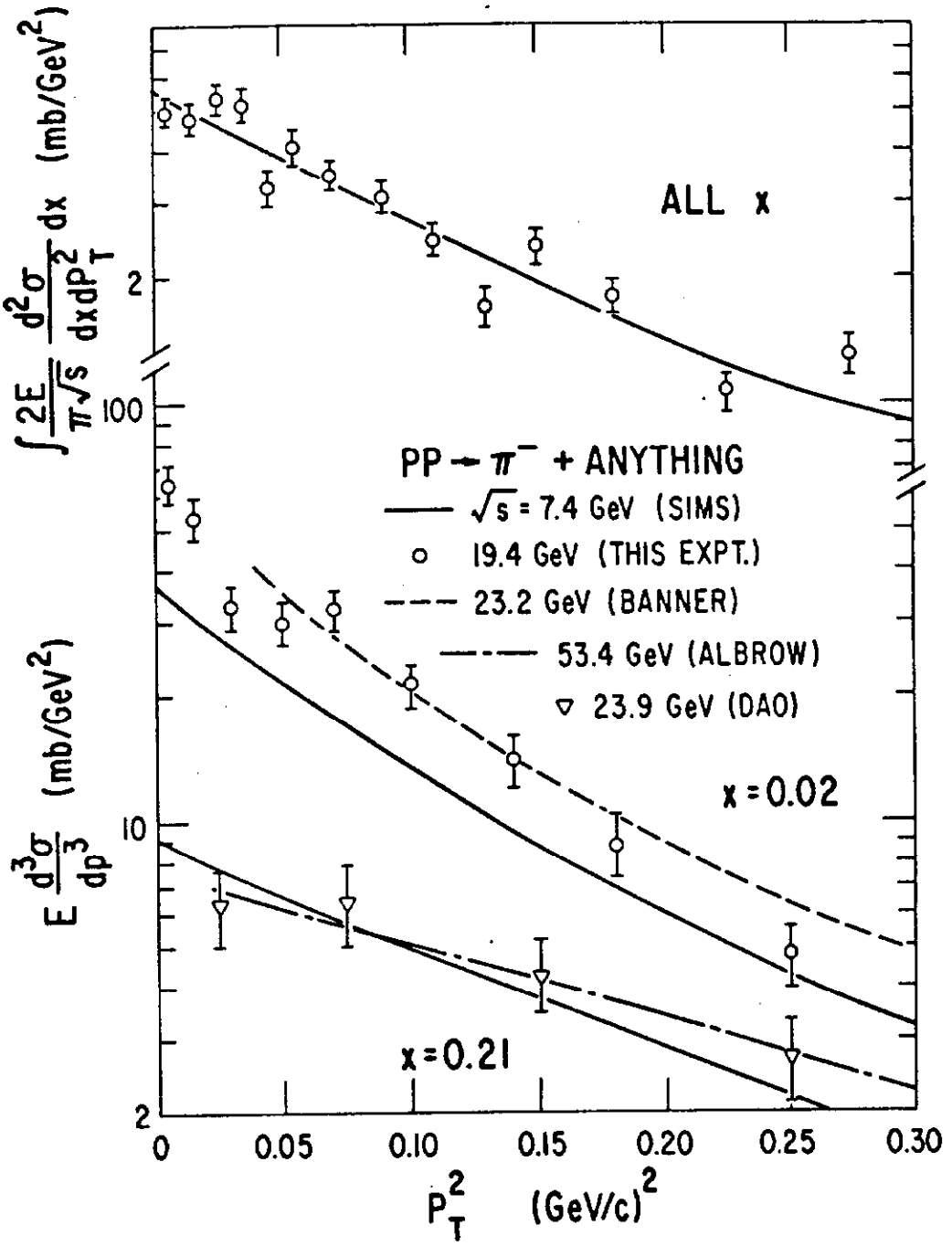

Fig. 4 p_T^2 distributions for π^- production.

From these data one observes the following features:

a) The $\pi^{\pm}$ cross sections at small $|x|$ and small p_T^2 [< 0.15 (GeV/c)^2] show a definite rise as the incident energy increases. Therefore, if any scaling limit exists in this region, it is approached from below.

b) For large x (~ 0.2) and large p_T^2 [> 0.15 (GeV/c)^2], scaling seems to be reached at relatively low energies (~ 20 GeV/c).

c) After integrating over all x, the p_T^2 distributions at 28.5 and 205 GeV/c are almost equal for π^- production.

In Fig. 5 we show the laboratory rapidity distributions for $\pi^{\pm}$ production in pp collisions. We note that scaling ($\sim \pm 10\%$) in the fragmentation region seems to occur at energies below 30 GeV/c. Our π^- data at 205 GeV/c show evidence for a plateau in the central region with a full width of the order of two units of rapidity.

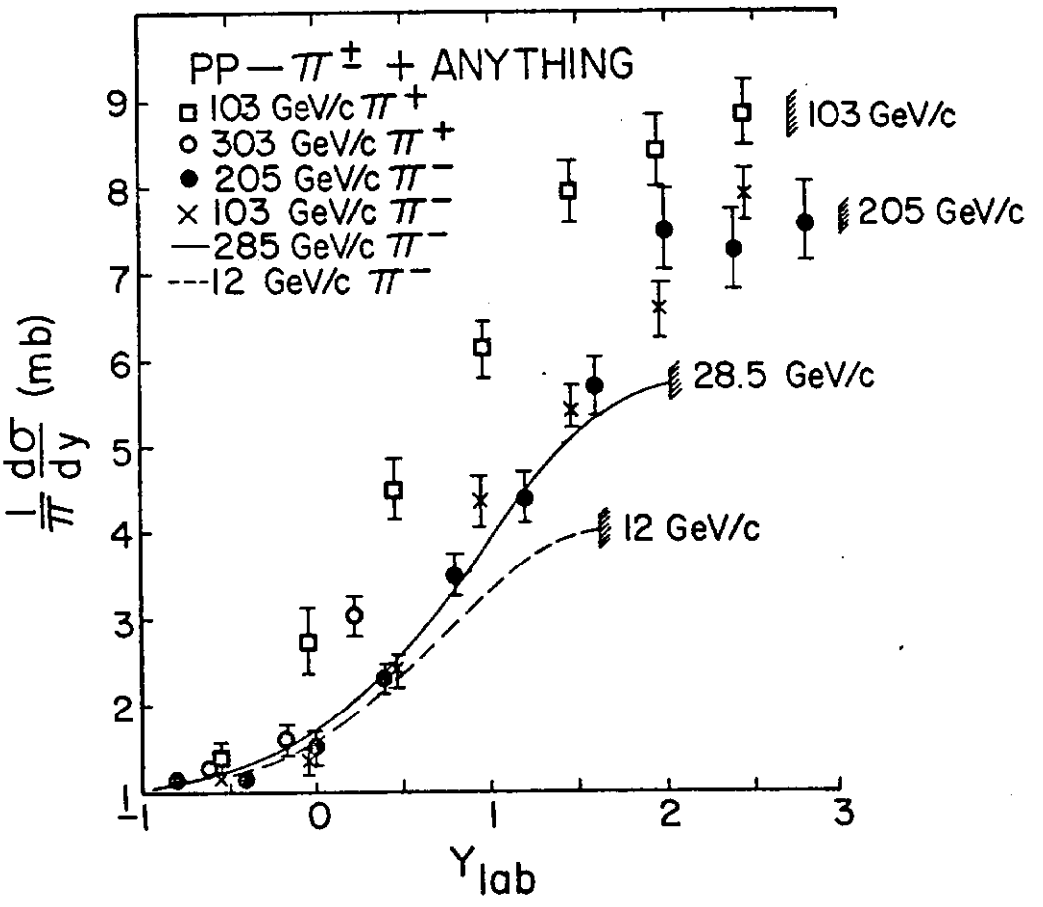

Fig. 5 Rapidity distributions for $\pi^{\pm}$ production.

As noted above, the cross section in the central region is increasing with energy. This is shown for π^- production in Fig. 6 which shows

$$\frac{1}{\pi} \int \frac{d^2\sigma}{dy\, dp_T^2} \Bigg|_{y = \text{const}} dp_T^2$$

as a function of $S^{-1/4}$ for different values of y = constant. The data at 90° CM are consistent with the $A + B\ S^{-1/4}$ behavior expected[7] from the Mueller-Regge phenomenology. We also see in Fig. 6 that the approach to scaling in the fragmentation region occurs at lower energies for smaller values of y. In fact, for $y_{lab} \lesssim 0.2$, the differential cross section at 12 GeV/c seems to be consistent with that at NAL energies.

THE STRUCTURE OF INDIVIDUAL EVENTS

Figure 7 shows the π^- rapidity distributions for various multiplicities. There is a definite trend for the width of the distribution to decrease as the multiplicity increases. To be more quantitative, the rms width of the highest multiplicity data shown in Fig. 7 is a factor of 1.32 ± 0.08 smaller than that of the lowest multiplicity data.

The average charged particle multiplicity in the forward hemisphere is shown in Fig. 8 as a function of the number of charged particles in the backward hemisphere. One observes that the average number in one hemisphere is independent of the charge multiplicity in the other hemisphere.

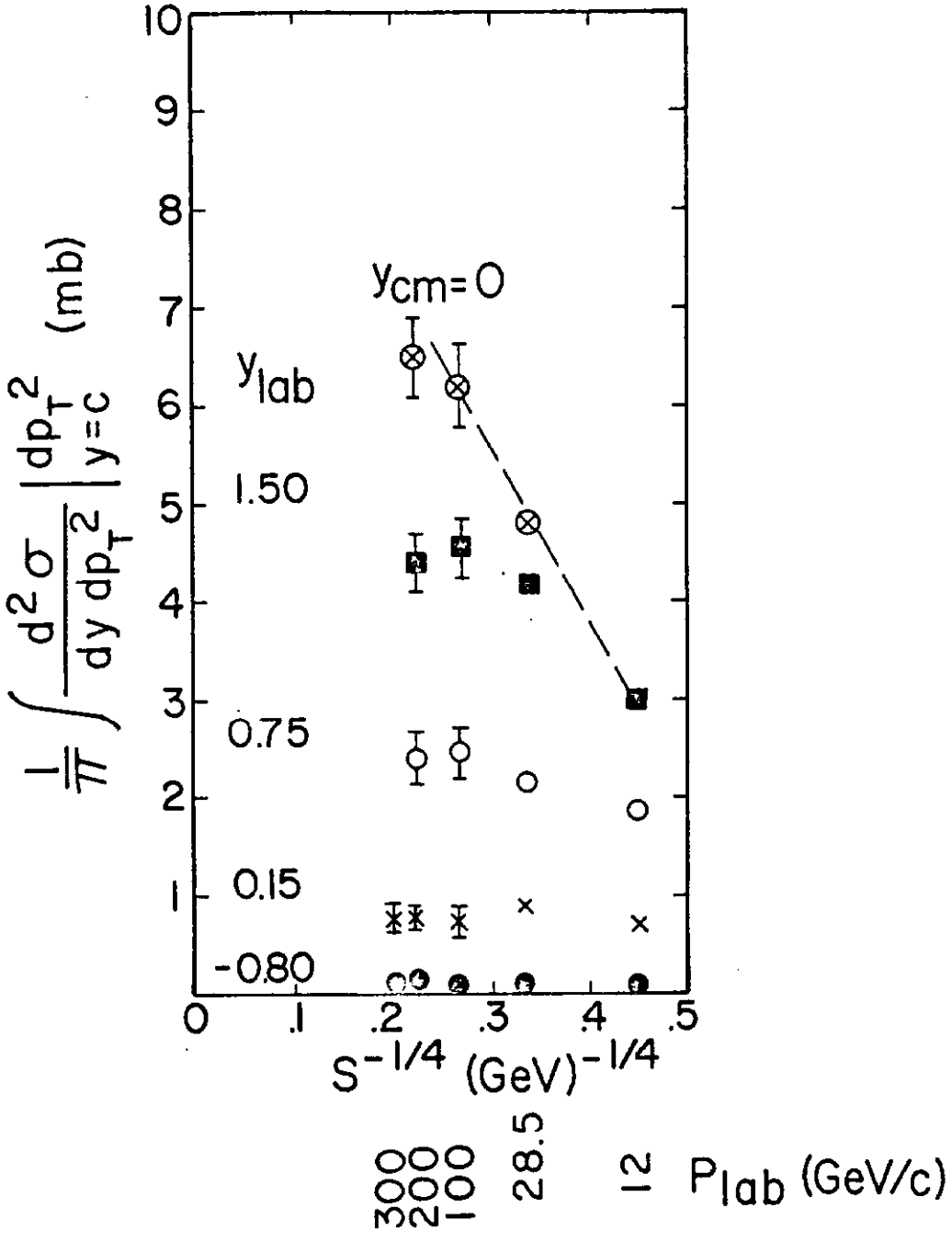

Fig. 6 π^- cross sections at fixed values of rapidity (after integrating over all p_T^2) as a function of $S^{-1/4}$.

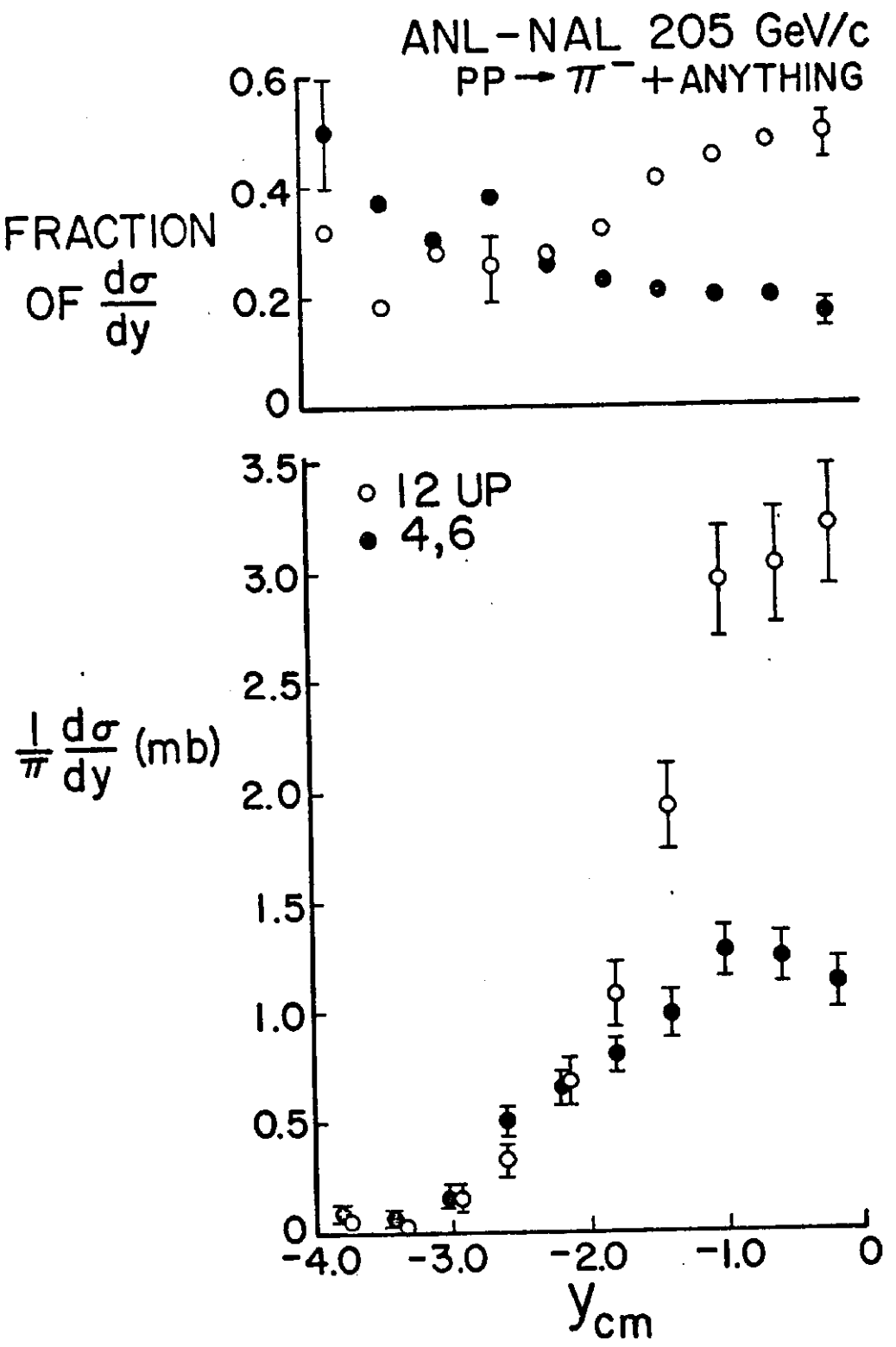

Fig. 7 π^- rapidity distribution for various multiplicities at 205 GeV/c.

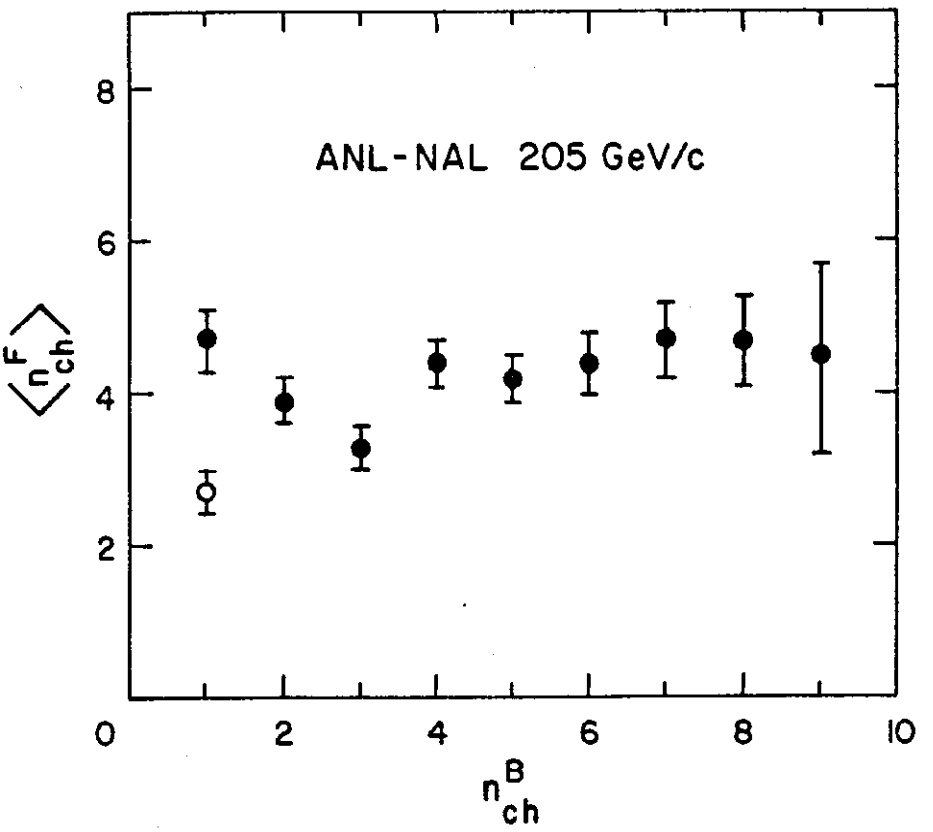

Fig. 8 Average charged particle multiplicity in the forward CM hemisphere as a function of the number of charged particles in the backward hemisphere. The open circle corresponds to including the inelastic two-prong events.

In Fig. 9 we show, for a given topology, the frequency of observing n_B particles in the backward CM hemisphere. Since pp collisions are symmetric on the average, the distributions have been folded about $n_B = n_{ch}/2$. This figure indicates that for all charged multiplicities above 4, the most likely configuration is a symmetric event with an equal number of charged particles in each hemisphere. This would favor a multiperipheral type of production process.[8] For the 4 prong event, there is some indication that the 1-3 split is most probable. This is probably related to diffractive type processes.

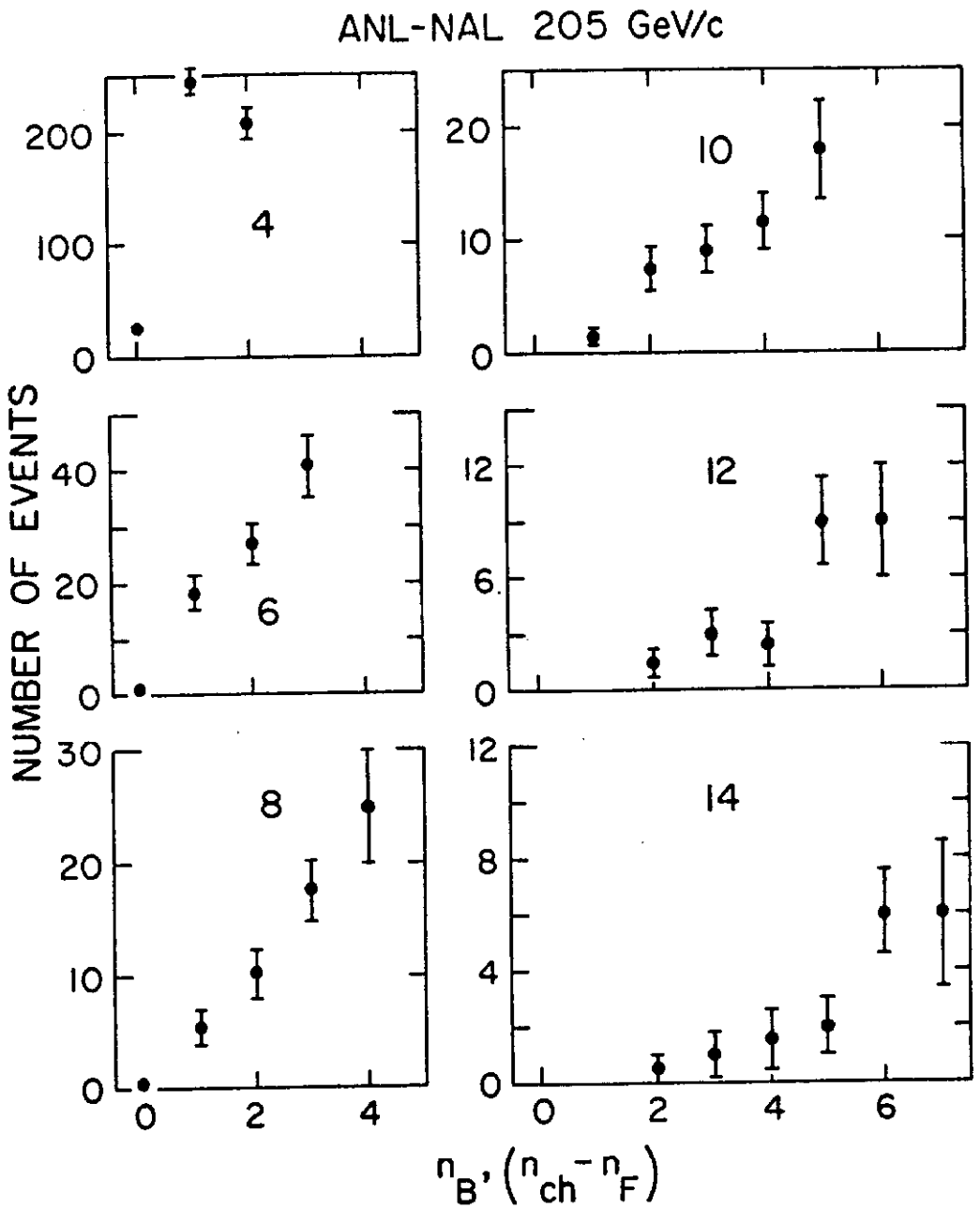

Fig. 9 The distribution of events, for a given multiplicity, as a function of the number of particles in the backward CM hemisphere.

It has been suggested[9] that the transfer of charge from one CM hemisphere to the other could be a distinguishing feature of various high energy multiparticle production processes. For pp collisions we define the charge transfer

$$u = \frac{1}{2}(Q_F - Q_B)_{\text{final}}$$

where Q_F (Q_B) is the net charge in the forward (backward) hemisphere following the interaction. Figure 10(a) shows the charge transfer distribution obtained at 205 GeV/c. We note that this distribution is symmetric about zero (as it should be for pp collisions) and that the maximum charge transfer observed is ± 3. Figure 10(b) shows the average value of u^2 evaluated for all events ($\bar{u}^2 = 0.94 \pm 0.08$) and the energy dependence of $\bar{u}^2$ expected for two different models.[9]

We now discuss the two particle correlations observed in 205 GeV/c pp collisions. Although the problems associated with not having particle mass identification are not severe, we shall use the variable $\eta = -\ell n \tan \theta_{\ell ab}/2$. We define

$$R_{12} = \frac{\sigma_{inel} \dfrac{d^2\sigma}{d\eta_1\, d\eta_2}}{\dfrac{d\sigma}{d\eta_1}\,\dfrac{d\sigma}{d\eta_2}} - 1$$

and in Fig. 11(a) we plot R_{12} as a function of $(\eta_2 - \eta_1)$ for fixed values of η_1 in the central region and for all charged particles. The data are consistent with an exponential falloff with a correlation length of 2 and a value of R_{12} $(\eta_1 = \eta_2 = 3) = 0.6 \pm 0.1$. Both of these values are consistent with ISR data[10] and again favor a multiperipheral production process. We further observe that the shape and magnitude of R_{12} are not dependent upon the exact value chosen as the center of the rapidity distribution.

Figure 11(b) shows R_{12} when η_1 is fixed at the edge of the plateau. As η_2 moves towards the center of the plateau the same exponential dependence is observed and indicates that R_{12} is invariant under translations provided that η_1, η_2 remain in the plateau region. Figure 11(b) also shows that as η_2 moves off the plateau, the decrease in R_{12} is faster. This may also be seen in Fig. 12 which shows that as η_1, η_2 become far apart, the correlation between them becomes zero and that as η_1, η_2 both approach

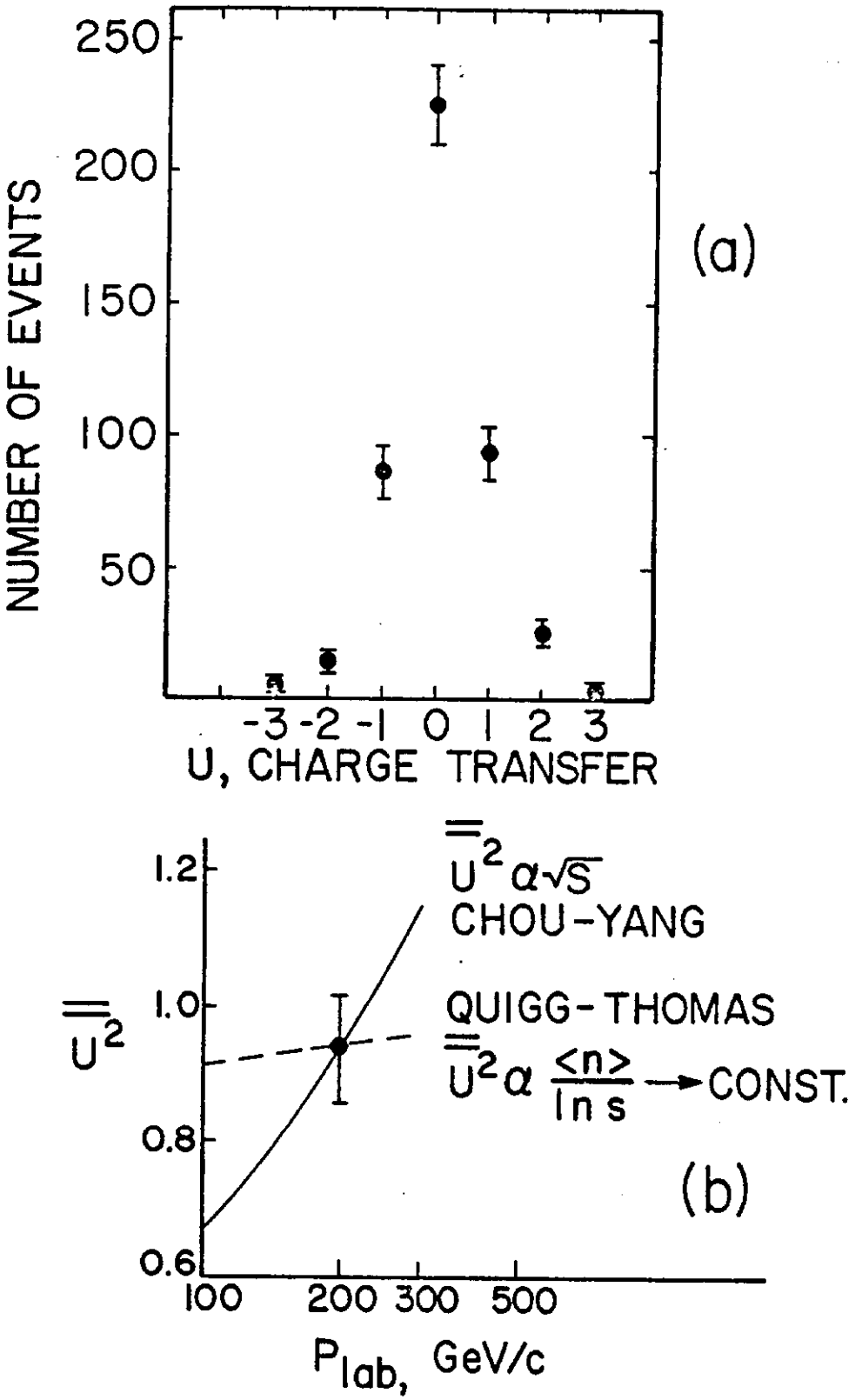

Fig. 10 (a) The charge transfer distribution at 205 GeV/c
(b) The average value of u^2 at 205 GeV/c.

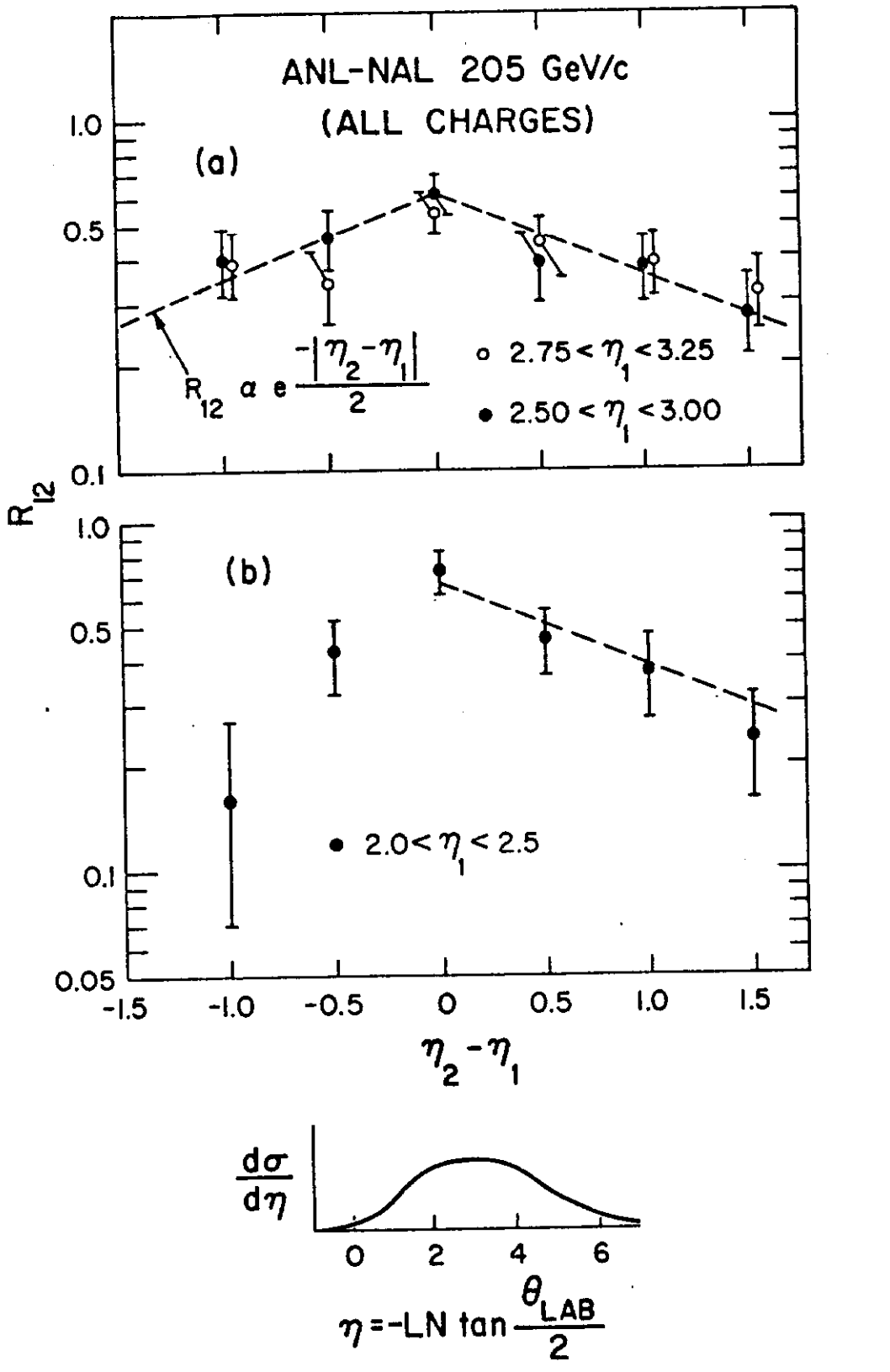

Fig. 11 Two particle correlation function at 205 GeV/c as a function of $\eta_2-\eta_1$ for all charges in (a) the central region and (b) the region near the edge of the rapidity plateau.

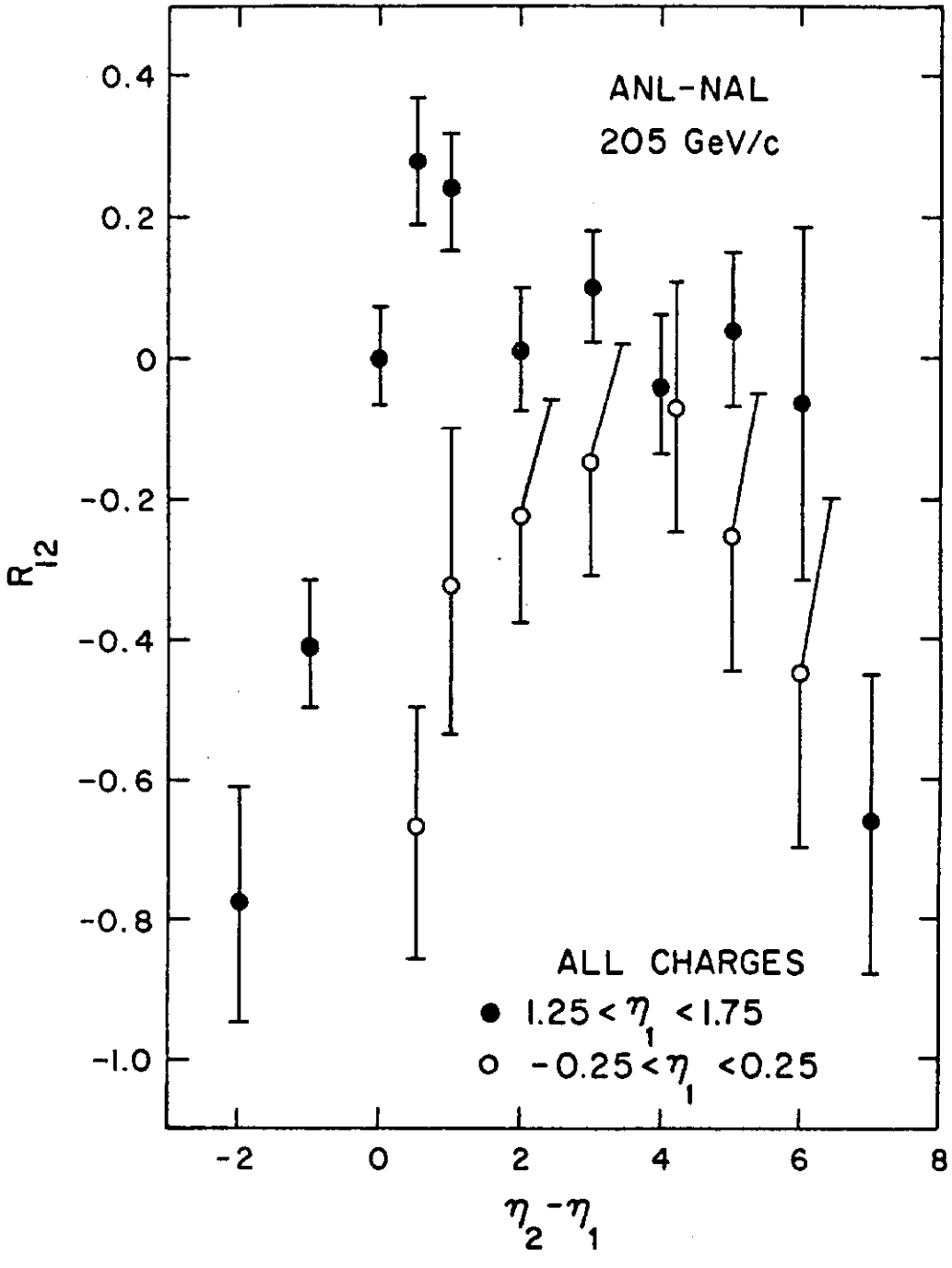

Fig. 12 Correlation function for η_1 fixed in the fragmentation region.

the fragmentation regions, the correlation becomes strongly negative. This is presumably indicative of the dominance of energy-momentum constraints.

Finally, Fig. 13 presents the correlation in the central region for like charges and shows (a) that the correlation for positives and for negatives is similar, (b) that R_{12} $(\eta_1=\eta_2=3) \sim 0.2$, and (c) that there is little dependence on $(\eta_2 - \eta_1)$.

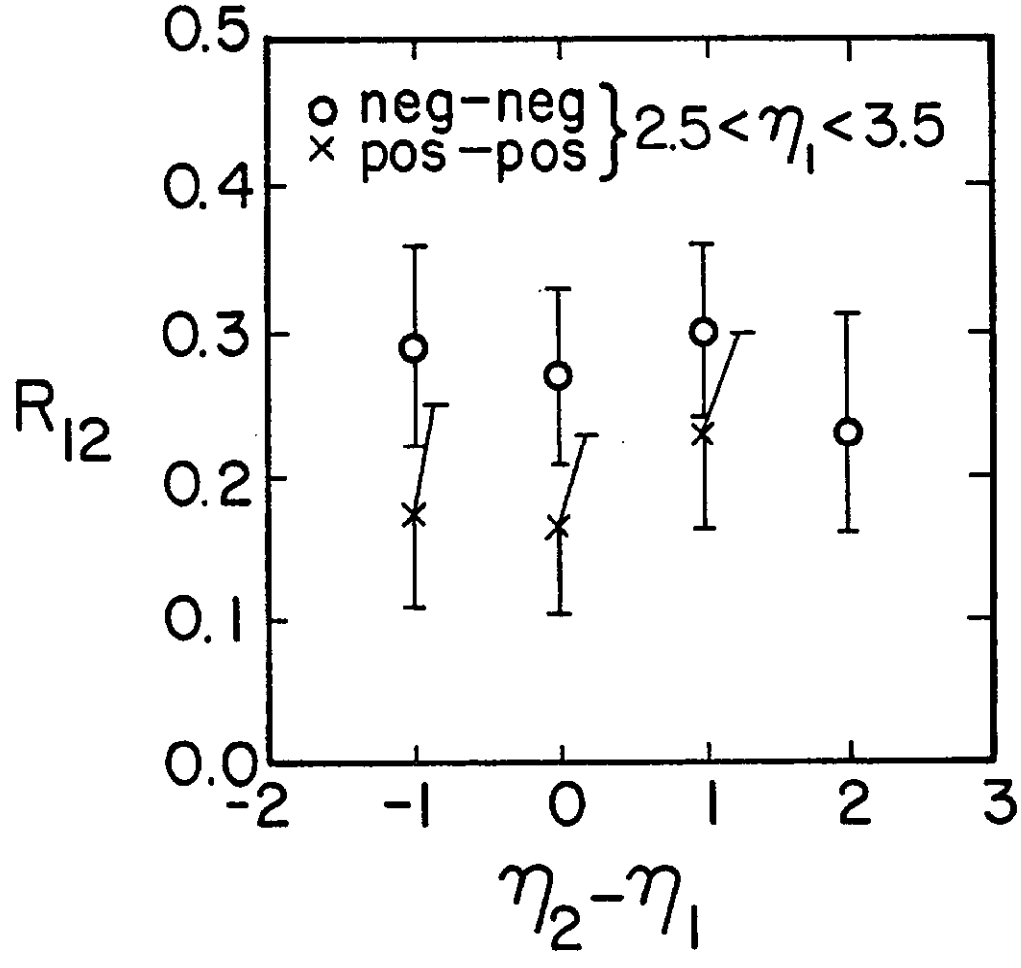

Fig. 13 Correlation function in the central region for like charges.

DIFFRACTIVE EXCITATION

In order to study possible diffractive effects present in 205 GeV/c pp collisions, we have measured the 2- and 4-prong events as well as all tracks identifiable as being protons with a momentum less than 1.4 GeV/c. The results of our latter measurements have been summarized[4] by Slattery. Figure 14 shows the proton t distributions in the 4-prong events for different ranges in the missing mass squared (MM^2) recoiling off the proton. One observes that the top plot, which corresponds to the low MM^2 peak, has a sharp t distribution with a slope parameter, $b = 9.3 \pm 1.1\ (GeV/c)^{-2}$, which is similar to that for elastic scattering. These events are therefore consistent with being diffractively produced by excitation of the beam proton. The higher ranges in MM^2 show less steep t distributions with slopes $\sim (5.0 \pm 1.5)\ (GeV/c)^{-2}$.

While being able to study beam excitation via MM^2 distributions, the bubble chamber also permits the study of the complementary process of target proton excitation via effective mass distributions. The $p\pi^+$ mass (using measured variables) for those 4-prong events where both the p and π^+ are identified is shown in Fig. 15(a). A significant $\Delta^{++}(1236)$ signal appears with a cross section of (0.51 ± 0.06) mb. The $p\pi^-$ mass spectrum, shown in Fig. 15(b), indicates that little $\Delta^0(1236) \rightarrow p\pi^-$ is produced. Figure 15(c) shows the $\Delta^{++}\pi^-$ mass distribution. One observes that this mass falls mostly below 3 GeV. Figure 15(d) shows that the MM^2 recoiling from these $\Delta^{++}\pi^-$ events has a strong tendency to peak at the nucleon mass. Furthermore, the distribution in four momentum transfer between target proton and $\Delta^{++}\pi^-$ (with mass less than 3 GeV) is shown in Fig. 16 and has a slope of $\sim 9.7\ (GeV/c)^{-2}$ in excellent agreement with Fig. 14. Hence, these events would appear to be examples of target excitation.

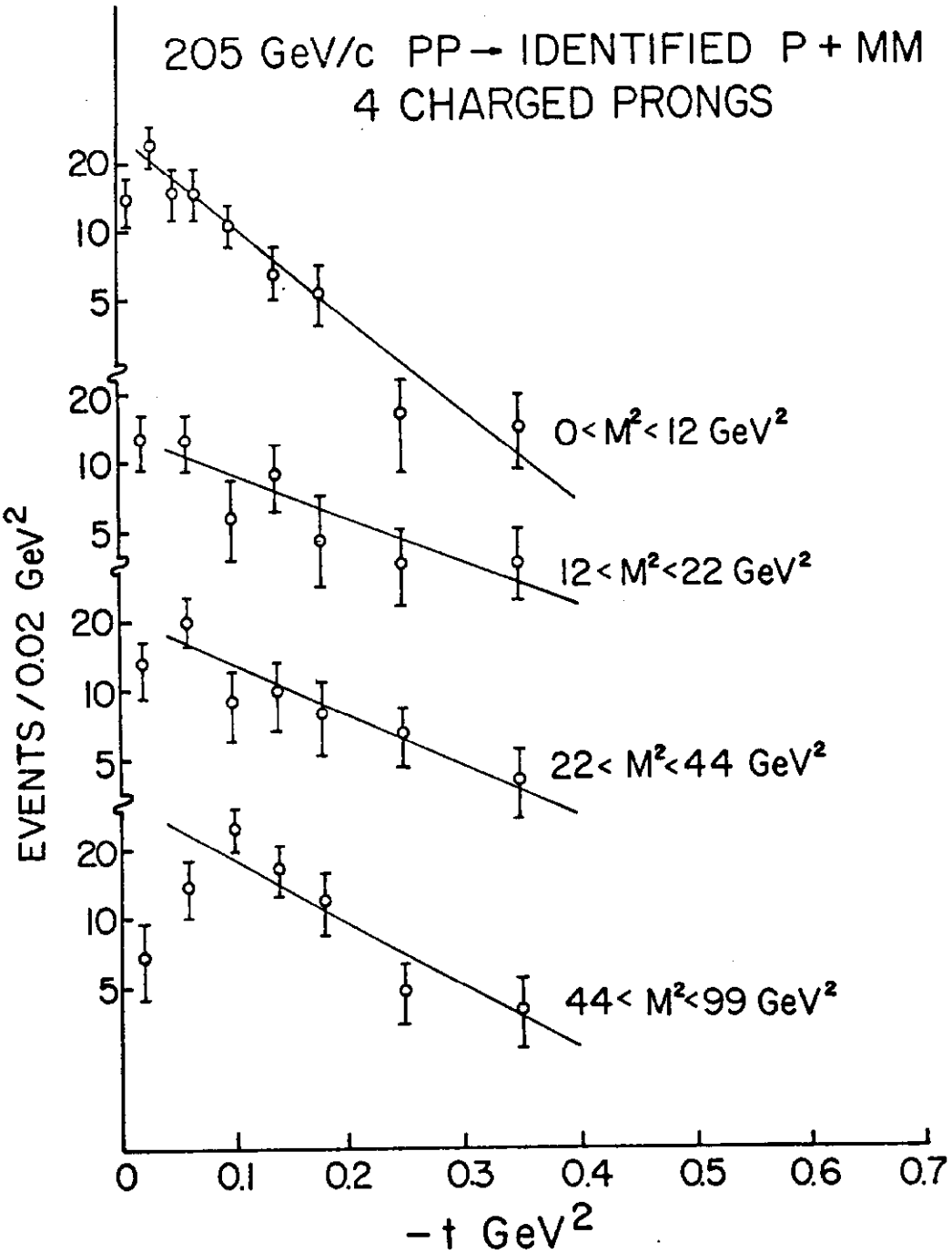

Fig. 14 Proton t distribution in the four-prong topology for different ranges in the missing mass recoiling off the proton.

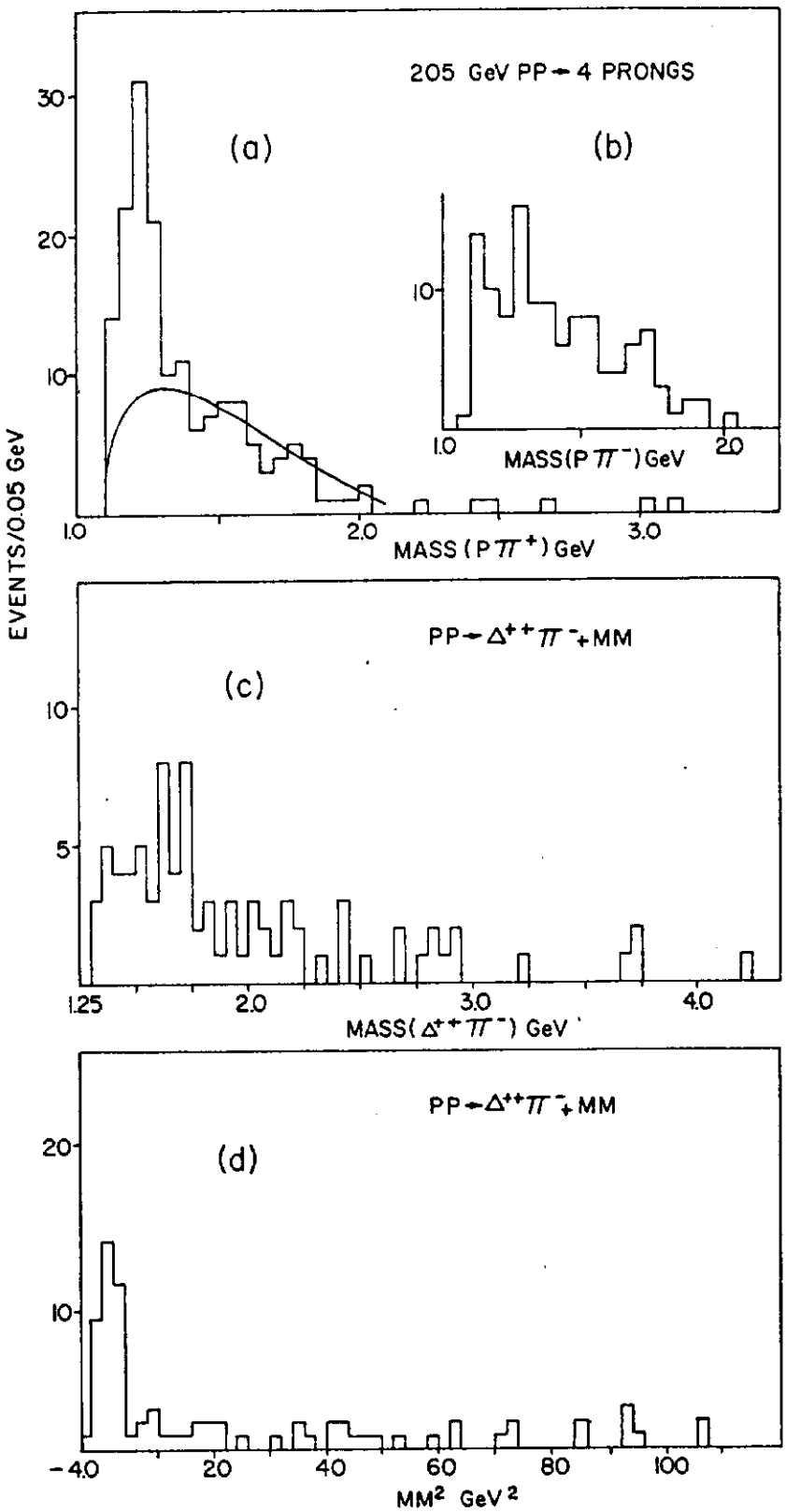

Fig. 15 Four-prong mass distributions: (a) $p\pi^+$ effective mass, (b) $p\pi^-$ effective mass, (c) $\Delta^{++}\pi^-$ effective mass, and (d) missing mass squared recoiling from the $\Delta^{++}\ \pi^-$ system.

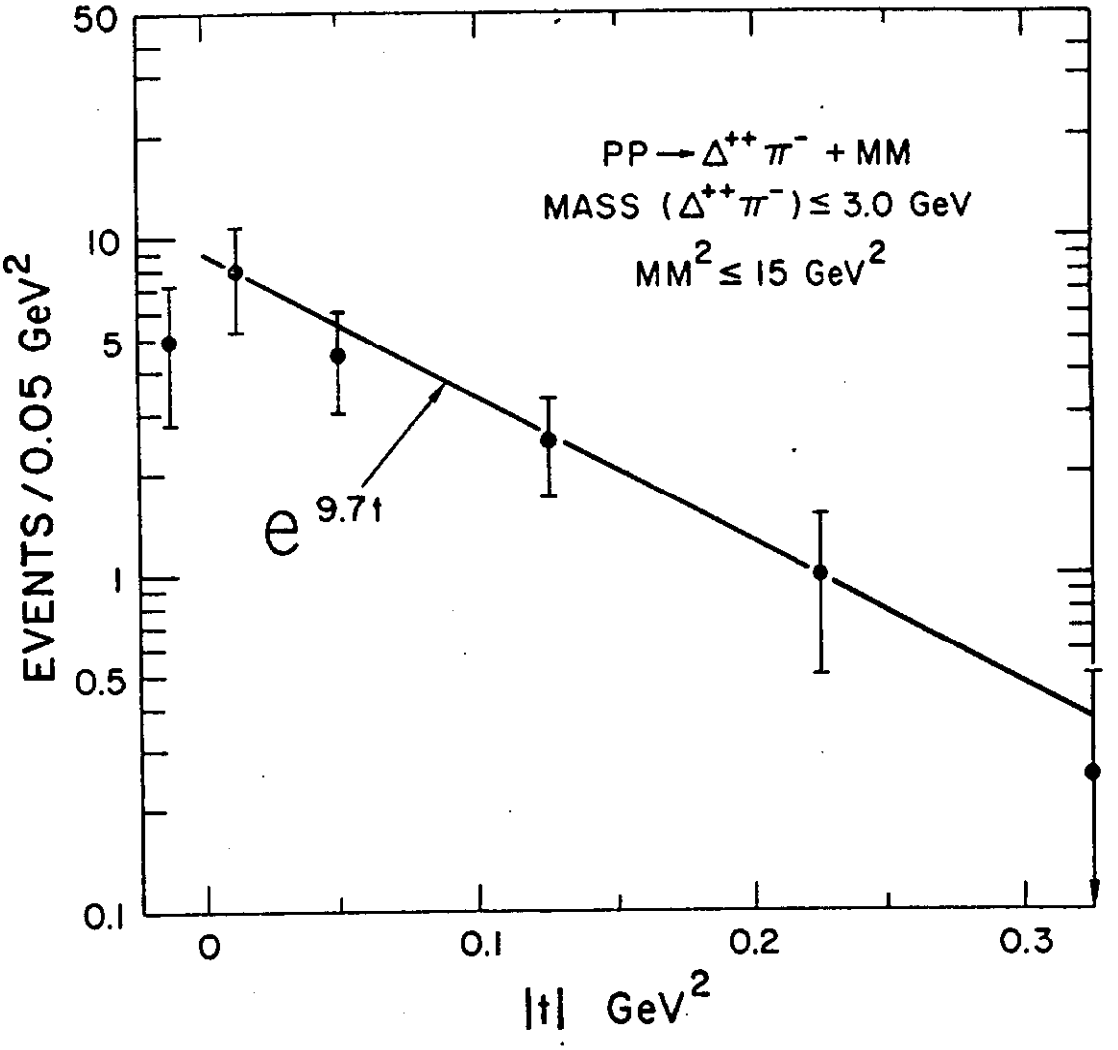

Fig. 16 Four momentum transfer between target proton and $\Delta^{++}\pi^-$.

REFERENCES

1. G. R. Charlton et al., Phys. Rev. Letters 29, 515 (1972).
2. For π production at 90° CM, the maximum laboratory momentum is 15 GeV/c, assuming a transverse momentum limit of 1.45 GeV/c.
3. For further details, see Y. Cho, R. Engelmann, T. Fields, L. Hyman, R. Singer, L. Voyvodic, and J. Whitmore, "Inclusive π^- Distributions from 205 GeV/c pp Interactions", ANL/HEP 7316, NAL-Pub-73/26-EXP (to be submitted to Phys. Rev. Letters).

4. P. Slattery, Proceedings of the Vanderbilt Conference; F. T. Dao et al., UCLA-NAL preprint: UCLA-1073, NAL-Pub 73/20 (1973).
5. 28.5 GeV/c: W. H. Sims et al., Nucl. Phys. B41, 317 (1972) and J. Hanlon, private communication; 24 and 12 GeV/c: H. J. Mučk et al., Phys. Letters 39B, 303 (1972), and V. Blobel, private communication.
6. ISR data: M. Banner et al., Phys. Letters 41B, 547 (1972); A. Bertin et al., Phys. Letters 38B, 260 (1972); M. G. Albrow et al., Phys. Letters 42B, 279 (1972); L. G. Ratner et al., "Inelastic Proton-Proton Scattering at Very High Energy", Proc. Rochester Meeting of APS/DPF, Rochester, 1971 (AIP, New York, 1971), p. 99.
7. T. Ferbel, Phys. Rev. Letters 29, 448 (1972).
8. S. Nussinov, C. Quigg, and Kiunn-Ming Wang, Phys. Rev. D6, 2713 (1972).
9. T. T. Chou and Chen Ning Yang, Phys. Rev. D7, 1425 (1973); C. Quigg and G. H. Thomas, ANL/HEP 7253, NAL-THY-96 (to be published in Phys. Rev.).
10. G. Belletini, Proceedings of the XVI International Conference on High Energy Physics, Chicago-Batavia (1972), to be published.